Food Hydrocolloids 147 (2024) 109371

Contents lists available at ScienceDirect

Food Hydrocolloids

journal homepage: www.elsevier.com/locate/foodhyd

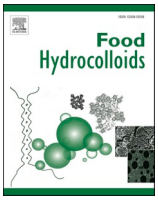

Chitin nanowhisker-containing photo-crosslinked antimicrobial gelatin films

Alaitz Etxabide [a,*], Daniel Mojío [b], Pedro Guerrero [a,c], Koro de la Caba [a,c], Joaquín Gómez-Estaca [b,**]

[a] BIOMAT Research Group, University of the Basque Country (UPV/EHU), Escuela de Ingeniería de Gipuzkoa, Plaza de Europa 1, 20018, Donostia-San Sebastián, Spain
[b] Institute of Food Science, Technology and Nutrition (CSIC), José Antonio Novais 10, 28040, Madrid, Spain
[c] BCMaterials, Basque Center for Materials, Applications and Nanostructures, UPV/EHU Science Park, 48940, Leioa, Spain

ARTICLE INFO

Keywords:
Active gelatin films
Photo-crosslinking
Chitin nanowhiskers
Nisin A
Antimicrobial activity

ABSTRACT

Nearly 57 Mt of food waste are generated annually in the EU for many reasons, for instance, because of microbial food spoilage. So, actions to reduce food loss and waste are needed and active packaging could offer a new approach towards this aim. In this study, antimicrobial gelatin films were prepared via the solution casting technique and their physicochemical, optical, mechanical, structural, barrier and antimicrobial properties were analysed. First, gelatin films were photo-crosslinked with riboflavin and the photo-curation time (0–4 h) was optimized. The optimal crosslinking time was 2 h since the solubility dropped down from 100% to 30% after 2 or 4 h of UV exposure. Then, 2 types of chitin nanowhiskers (CNWs) obtained via acid hydrolysis (AH) and TEMPO-mediated oxidation processes were added in 2 concentrations (2 and 4 wt %) into the film-forming solution (FFS) as reinforcements before film photo-crosslinking. The AH-CNW at 4 wt % was chosen as an optimal CNW type and concentration because they further decreased the solubility (~24%) of films and improved mechanical properties up to values similar to those of commercially available synthetic packaging films. Finally, various concentrations (0, 7.5, 15 and 30 wt %) of the antimicrobial compound (Nisin A®) were added to the optimized formulation which showed good antimicrobial properties on both spoilage and pathogen strains, as well as over the native microbiota of chilled sea bream fillets, sliced cold-smoked salmon and chicken breast fillets. The developed films displayed promising properties as antimicrobial packaging for myosistem foods.

1. Introduction

In the EU, nearly 57 million tonnes of food waste are generated yearly and it is estimated that around 10% of food made available to EU consumers may be wasted (European Commission, 2022). Food loss occurs for many reasons, for instance, because of microbial growth of both spoilage and pathogenic microorganisms, making food unsuitable for consumption. Therefore, although actions to reduce food loss and waste are being taken (the Farm to Fork strategy, the Sustainable Development Goals (SDG number 12)), new tactics and strategies must be explored, and active packaging could offer a new approach towards this aim (Fadiji, Rashvand, Daramola, & Iwarere, 2023; Packaging Europe, 2022).

Active packaging systems interact with the environment of the packaged food or with the food itself during the food preservation period. This is so because these materials have been designed to incorporate active agents and functional additives intended to be released into the food or absorbed into or from the packed food or the environment surrounding the food. The interactions occur via (in)direct contact of the packaging with food or the release of active agents from the packaging into the food, and these agents carry out several functions associated with food preservation, such as O_2 scavenging or microorganism growth reduction. These are very important properties for preserving the safety and sensory properties of packaged foods as well as maintaining their quality for longer times, which, in turn, help reduce food waste via food spoilage reduction (Etxabide, Garrido, Uranga, Guerrero, & de la Caba, 2018; Fadiji et al., 2023; Soltani Firouz, Mohi-Alden, & Omid, 2021; Vilela et al., 2018).

Food spoilage caused by microbial activity or growth is the most common cause of food degradation, which makes the food inappropriate

* Corresponding author.
** Corresponding author.
E-mail addresses: alaitz.etxabide@ehu.eus (A. Etxabide), joaquin.gomez@csic.es (J. Gómez-Estaca).

https://doi.org/10.1016/j.foodhyd.2023.109371
Received 7 July 2023; Received in revised form 26 September 2023; Accepted 28 September 2023
Available online 29 September 2023

for consumption and therefore, it ends up as food loss. In this matter, antimicrobial active packaging systems inhibit or prevent microbial growth, consequently delaying food spoilage and extending food shelf life (López-Carballo, Gómez-Estaca, Catalá, Hernández-Muñoz, & Gavara, 2012). While the first active packaging development systems consisted of the incorporation of the active substances into a sachet or similar, packaging systems including the active compounds into the bulk of films, as coatings, or immobilized at the films' surfaces are the most interesting ones (López-Carballo et al., 2012). Among many antimicrobial agents, bacteriocins are antimicrobial peptides produced by bacteria that exhibit excellent antibacterial properties and one example is nisin, a *Lactococcus lactis subs*.-produced polypeptide. The mechanism of action of nisin refers to its ability to disrupt the bacterial membrane integrity and it shows activity against a broad range of Gram-positive bacteria, including many foodborne pathogens and spoilage bacteria (e.g., *Micrococcus*, *Lactococcus*, *Leuconostoc*, *Lactobacillus*, *Pediococcus*, *Listeria*, and *Staphylococcus*). This polypeptide, recognized as a biologically safe food preservative by the FAO and WHO organizations and approved to be used as a natural antimicrobial agent in foodstuffs in more than 50 countries, is widely used in the food industry as a safe and natural preservative, being the inhibition of foodborne pathogens and the prevention of spore germination the two major roles of nisin in the industry (Bahrami, Delshadi, Jafari, & Williams, 2019; Popa et al., 2022; Zehetmeyer et al., 2016).

When it comes to selecting a matrix to incorporate the antimicrobial agent and developing active food packaging, expanding the use of biopolymers in packaging is one way to overcome the use of petroleum-based polymeric packaging which is piling up everywhere in the environment (Westlake et al., 2023). Fish gelatin is a renewable (extracted from marine waste), biodegradable, economical and abundant biopolymer (a protein), which has shown excellent film-forming capacity, transparency as well as both UV-light and oxygen barrier properties. Therefore, due to its interesting properties, gelatin has been considered a promising biopolymer for green food packaging development and a possible alternative to petroleum-based food packaging materials. However, some characteristics such as water stability and mechanical properties of gelatin must be improved before incorporating active agents and being used as an active food packaging material (Hosseini & Gómez-Guillén, 2018).

The water stability of gelatin can be improved via crosslinking (Garavand, Rouhi, Razavi, Cacciotti, & Mohammadi, 2017). Among many crosslinkers and crosslinking processes, photo-induced crosslinking is an environmentally friendly approach that has recently gained significant research attention (Lee, Lim, Lee, Park, & Lee, 2023). The light-induced chemical reactions require a photoinitiator to improve the water stability of biopolymers, and riboflavin (vitamin B2) is a natural and food-grade photo-active agent used for UV-induced crosslinking of biopolymers (Li, Sheng, Sun, & Wang, 2020). In this study, the influence of UV-induced photo-crosslinking on gelatin film characteristics was assessed as a first characterization step.

Regarding the improvements of gelatin films' mechanical properties, the inclusion of nanostructures as reinforcing fillers is a promising way to enhance the mechanical performance of biopolymers (Hosseini & Gómez-Guillén, 2018). Among natural nanomaterials, chitin nanowhiskers (CNWs) are organic, renewable (obtained from crab and shrimp shells) and biodegradable biopolymers (polysaccharides) which are increasingly being used in packaging materials as reinforcing agents (Liao, Zhou, Hou, Zhang, & Huang, 2023). In this study, the influence of differently-extracted CNWs and their concentrations on the properties of photo-crosslinked gelatin films were analysed, as a second characterization step.

After improving the water stability and mechanical properties of gelatin films, the incorporation of different Nisin A® concentrations was carried out to develop active films with antimicrobial properties. In sum, the objectives of this work were: i) the optimization of photo-crosslinking time to improve the water stability of gelatin films; ii) the selection of the optimal CNW type and concentration based mainly on the mechanical properties of the films; and iii) the assessment of the effect of various Nisin A® concentration addition on the properties of photo-crosslinked CNW-containing gelatin films for active food packaging applications.

2. Materials and method

2.1. Materials and strains

Type A codfish gelatin (Weishardt, Liptovsky Mikulas, Slovakia), chitin from shrimp shells (Glentham Life Sciences, Corsham, UK), riboflavin (vitamin B2) and glycerol (both from Sigma Aldrich, Barcelona, Spain), and Nisin A® (nisin (w/w) $\geq$ 2.5% and sodium chloride (w/w) $\leq$ 75%; Handary Brussels, Belgium) were used to formulate films. Culture media were from Scharlau (Barcelona, Spain) (plate count agar and iron agar) and Oxoid (Basingstoke, UK) (brain heart infusion broth-BHI). Buffered peptone water was also from Oxoid. All other reagents were of analytical grade and acquired from Sigma-Aldrich (Barcelona, Spain) or Panreac (Madrid, Spain). The strains used for antimicrobial activity study were acquired from the Spanish Type Culture Collection (CECT): *E. coli K12* (CECT 433), *B. cereus* (CECT 148), *B. thermosphacta* (CECT 847), *P. fluorescens* (CECT 4898), *A. hydrophila* (CECT 839) and *P. phosphoreum* (CECT 4192), and the food samples acquired at a local market.

2.2. CNWs preparation

Two types of CNWs were obtained. The first group of CNWs were prepared through acid hydrolysis (AH), as indicated in our previous work (Etxabide, Kilmartin, Maté, & Gómez-Estaca, 2022), and were named AH-CNWs. The second group of CNWs were prepared through TEMPO-mediated oxidation as described by Fan and colleagues (Fan, Saito, & Isogai, 2008), with slight modifications. Briefly, 10 g of chitin were suspended in 1000 mL of distilled water containing TEMPO (2,2,6,6-Tetramethylpiperidine 1-oxyl, 2,2,6,6-Tetramethyl-1-piperidinyloxy, free radical) (0.16 g) and sodium bromide (1 g). Then, 7.5 mmol of NaClO per gram of chitin was added and the pH was maintained at 10 under continuous addition of 1 M NaOH using a pH-Stat titration system (Metrohm 916 Ti-Touch system, Madrid, Spain). When oxidation concluded (no more alkali was needed to add to maintain the pH at 10), pH was adjusted to 7 with 0.5 M HCl and the mixture was centrifuged (12000 g/10 min/20 °C). The precipitate was resuspended in distilled water and dialyzed against distilled water for 3–4 days using a 12–14, 000 Da molecular weight cut membrane (Medicell Membranes Ltd, London, UK). Then, 200 mL aliquots were sonicated for 5 min (1 min on/1 min off cycles) using a Qsonica equipment (Q700 model, Newton, CT, USA) set at 95% amplitude. The samples were immersed in a water/ice bath to avoid overheating. These CNWs were named TEMPO-CNWs. The morphology of both samples was observed by transmission electron microscopy (TEM) in a JEOL JEM-1230 microscope (Fig. S1). For that, samples were previously adsorbed on glow-discharged carbon-coated grids and stained with 2% uranyl acetate. Grids were observed at 100 kV and a nominal magnification of 50 K. Images were taken under low dose conditions with a CMOS Tvips TemCam-F416 camera. The size (average length and width $\pm$ standard deviation) of CNWs was measured using the Image J software.

2.3. Film preparation

The pH of the gelatin solution was adjusted to 3 during the film preparation process due to: i) riboflavin degradation increases by around 80-fold in alkaline media (Wong, Rhodes, & Dessent, 2021); and ii) the solubility and molecular stability of Nisin A® is pH dependent; Nisin A® is highly soluble and stable at acidic pHs (Fael & Demirel, 2020; Müller-Auffermann, Grijalva, Jacob, & Hutzler, 2015). In this

study, Nisin A® containing NaCl in high amounts was used since the presence of the salt may allow both to prolong nisin activity (Holcapkova et al., 2017) as well as provide greater antimicrobial protection as observed in some food products (Wu et al., 2023).

2.3.1. Effect of photo-crosslinking time

Riboflavin-crosslinked gelatin films were prepared using the casting method. An amount of 5.0 g of gelatin were dissolved in 80 mL Type II water (Autwomatic Plus 1 + 2, Wasserlab) for 30 min at 60 °C under continuous stirring (250 rpm) to obtain a homogeneous blend. Then, the pH of the solution was adjusted to 3 with 1 N HCl. Meanwhile, 0.2 wt % of riboflavin (Wang, K. et al., 2017) and 10 wt % of glycerol (Etxabide et al., 2022) (both on a gelatin dry weight basis) were dissolved in 20 mL Type II water and treated with an ultra-turrax (T25 digital, IKA) at 8,000 rpm for 5 min at 21 °C. After that, both solutions were mixed, and the resulting blend was maintained at 60 °C for 30 min under stirring. Finally, 5.5 g of the blend were poured into each Petri dish (ø 60 mm), photo-crosslinked (4 lamps, 36 W, 370–405 nm, Domotek, Spain) for 0, 0.5, 1, 2 or 4 h, and left to dry and form the film in an oven at 40 °C for 24 h. The following designation was used for naming each system as a function of photo-crosslinking time: t0 (control1), t0.5, t1, t2 and t4 for crosslinking times of 0, 0.5, 1, 2 and 4 h, respectively.

2.3.2. Effect of CNWs addition

Gelatin-based films with different CNW types (AH-CNWs and TEMPO-CNWs) and contents (2 and 4 wt %, on a gelatin dry weight basis) were prepared using casting as indicated in the 2.3.1 section. A proportion of 2 and 4 wt % CNWs (AH and TEMPO), 0.2 wt % of riboflavin and 10 wt % of glycerol (all on a gelatin dry weight basis) were dissolved in 20 mL Type II water and treated with an ultra-turrax at 8,000 rpm for 5 min at 21 °C before adding the mixture to the previously prepared acidic (pH 3) gelatin solution (5 g/80 mL). The resulting blend was maintained at 60 °C for 30 min under stirring. Finally, 5.5 g of the FFS were poured into each Petri dish (ø 60 mm), photo-crosslinked for 2 h and left to dry and form the film in an oven at 40 °C for 24 h. The following designation was used for naming each system as a function of CNW type and content: t2 (0% CNWs, control2); t2-AH2 and t2-AH4 (2 and 4 wt % AH-CNWs); and t2-TEMPO2 and t2-TEMPO4 (2 and 4 wt % TEMPO-CNWs).

2.3.3. Effect of Nisin A® addition

t2-AH4 gelatin-based films with different Nisin A® contents were prepared using casting as indicated in the 2.3.2 section. Nisin A® (0, 7.5, 15 and 30 wt %), 4 wt % AH CNWs, 0.2 wt % of riboflavin, and 10 wt % of glycerol (all on a gelatin dry weight basis) were dissolved in 20 mL Type II water and treated with an ultra-turrax at 8,000 rpm for 5 min at 21 °C before adding the mix to the previously prepared acidic (pH 3) gelatin solution (5 g/80 mL). The resulting blend was maintained at 60 °C for 30 min under stirring. Finally, 5.5 g of the FFS were poured into each Petri dish (ø 60 mm), photo-crosslinked for 2 h and left to dry and form the film in an oven at 40 °C for 24 h. The following designation was used for naming each system as a function of Nisin content: t2-AH4 (0% Nisin A®, control3), t2-AH4-Ni7.5 (7.5% Nisin A®), t2-AH4-Ni15 (15% Nisin A®) and t2-AH4-Ni30 (30% Nisin A®).

A summary of all films prepared in this study along with their designation can be found in Table 1.

2.4. Film characterization

2.4.1. Film thickness

A Mitutoyo hand-held QuantuMike digimatic (Unceta, Elgoibar, Spain) micrometre was used to measure film thickness to the nearest 0.001 mm. Twelve samples were measured for each system (n = 12). The films were 108.13 ± 27.13 μm thick and no significant differences were observed in thickness with the photocrosslinking time extension or the addition of CNWs and Nisin A®.

Table 1
A summary of the prepared films and their designation as a function of crosslinking time ($t_{crosslinking}$), type and concentration of chitin nanowhisker (CNW), and Nisin A® content.

Film designation	$t_{crosslinking}$ (h)	CNW type	CNW content (wt %)	Nisin A® content (wt %)
t0 (control1)	0	–	0	0
t0.5	0.5	–	0	0
t1	1	–	0	0
t2 (control2)	2	–	0	0
t4	4	–	0	0
t2-AH2	2	AH	2	0
t2-AH4 (control3)	2	AH	4	0
t2-TEMPO2	2	TEMPO	2	0
t2-TEMPO4	2	TEMPO	4	0
t2-AH4-Ni7.5	2	AH	4	7.5
t2-AH4-Ni15	2	AH	4	15
t2-AH4-Ni30	2	AH	4	30

2.4.2. Colour

A Minolta CR-400 Chroma Meter was used to measure colour parameters (CIELAB scale): L* = 0 (black) to L* = 100 (white), −a* (greenness) to +a* (redness), and −b* (blueness) to + b* (yellowness). Films were deposited on white paper (L* = 92.31, a* = 0.82, and b* = −2.82) before making the measurements. Twelve samples were measured for each system (n = 12). The total colour difference (ΔE*), in reference to the control in each film preparation section (2.3.1-2.3.3), was measured as follows:

$$\Delta E^* = \sqrt{(\Delta L^*)^2 + (\Delta a^*)^2 + (\Delta b^*)^2}$$

2.4.3. Light absorbance

A UV Multiskan SkyHigh (Madrid, Spain) ultraviolet–visible (UV–Vis) spectrophotometer was used to measure the light absorbance of films from 200 to 800 nm and their transparency at 600 nm. Three specimens were tested for each composition (n = 3). The transparency (T) was calculated as follows:

$$T = \frac{A_{600}}{x}$$

where A_{600} is the absorbance value at 600 nm and x is the average thickness (mm) of the films.

2.4.4. Attenuated total reflectance fourier transform infrared (ATR-FTIR) spectroscopy

A Bruker ALPHA II FTIR spectrometer (Barcelona, Spain) was used to obtain ATR-FTIR spectra from 4000 to 750 cm^{-1} with a resolution of 4 cm^{-1} and 32 scans per sample. Three samples were measured for each system (n = 3).

2.4.5. X-ray diffraction (XRD)

A PANalytic Xpert Pro (Madrid, Spain) equipment with a diffraction unit and Cu-Kα (λ = 1.5418 Å) as a radiation source was used to carry out XRD analysis at 40 kV and 40 mA from 2θ = 5.0–50.0° (n = 2).

2.4.6. Solubility of films

Five specimens (n = 5) of each film were weighed (W_0) and immersed into 10 mL of Type II water (aqueous food simulant) at 20 °C for 24 h. After that, specimens were taken out of the water and left to dry in an oven at 40 °C for 24 h before reweighing (W_t). The solubility of films was calculated by the following equation:

$$Solubility\ (\%) = \frac{(W_0 - W_t)}{W_0} \times 100$$

The release of riboflavin from films into Type II water was analysed after the solubility test by introducing the food simulant in quartz

cuvettes at UV–Vis spectrophotometer and recording wavelengths from 200 to 800 nm. Three tests (n = 3) were carried out for each composition.

2.4.7. Tensile test

Mechanical properties were measured with a Texturometre TA.XT plusC (Stable microsystems), according to ASTM D882-02 (ASTM D882-02, 2002). Films were cut into bone-shaped samples of 4.75 mm × 22.25 mm, and the tensile test was conducted with a load cell of 50 N and a crosshead rate of 5 mm/min. Five samples were measured for each system (n = 5). Tensile strength (TS), elongation at break (EB) and elastic modulus (E) were evaluated from the measurements.

2.4.8. Scanning electron microscopy (SEM)

A Hitachi S-4800 (Madrid, Spain) SEM was used with an acceleration voltage of 5 kV to visualise the surface and cross-section morphologies of the films. Samples were placed in a metallic stub and coated with gold under a vacuum in an argon atmosphere.

2.4.9. Water vapour permeability (WVP)

A Labthink PERME™ W3/0120 instrument was employed to determine WVP gravimetrically (n = 2) at 38 °C and 90% RH, according to ASTM E96-00 (ASTM E96-00, 2000). WVP was determined as follows:

$$WVP\left(\frac{g}{cm \bullet s \bullet Pa}\right) = \frac{(G \times L)}{(t \times A \times \Delta P)}$$

where G is the weight change (g), L is the film thickness (mm), t is time (h), A is the test area (cm^2) and ΔP is the partial pressure difference of water vapour across the film.

2.4.10. Antimicrobial activity

The antimicrobial activity of the films was assayed over some selected spoilage or pathogen (or its subrogate) microorganisms as well as over the spoilage microbiota of minced beef meat, sea bream fillets, sliced cold-smoked salmon and chicken breast fillets stored (5 °C) for 7 (beef, sea bream, chicken) or 20 (cold-smoked salmon) days in aerobic conditions (open packages). An amount of 30 g of each food sample was aseptically weighed and homogenized with 70 mL of sterile 0.1% buffered peptone water in a stomacher blender. Strains from a collection stored at −80 °C in BHI broth with 25% glycerol were grown in BHI broth (supplemented with 1% NaCl for *P. phosphoreum*) at 37 °C (*E. coli* K12, *B. cereus*), 30 °C (*A. hydrophila, P. fluorescens*), 25 °C (*B. thermosphacta*) or 15 °C (*P. phosphoreum*). Spread plates of PCA media were prepared with 100 μL of each bacterial suspension (both collection microorganisms and food sample homogenates), except for *P. phosphoreum* which was seeded onto Iron Agar plus 1% NaCl plates. Circular pieces (13 mm in diameter) of each film containing 0, 7.5, 15 and 30 wt % of Nisin A® were placed onto the spread plates and incubated at 37 °C for 24 h (*E. coli, B. cereus*), at 25 °C for 48 h (*B. thermosphacta*), at 30 °C for 48 h (*P. fluorescens*) or 72 h (*A. hydrophila*) and at 15 °C for 72h (*P. phosphoreum*). Food sample homogenates were incubated at 30 °C for 24 h. Inhibition areas were measured using a Scan 1200 automatic colonies counter (Interscience, France) and expressed in millimetres (mm).

2.4.11. Statistical analysis

Data were subjected to one-way analysis of variance (ANOVA) using an SPSS computer program (SPSS Statistic 25.0). Post hoc multiple comparisons were determined by Tukey's test with the level of significance set at $P < 0.05$.

3. Results and discussion

3.1. Photo-crosslinking time selection

The photo-crosslinking reaction between gelatin and riboflavin was assessed employing different techniques and tests (Fig. 1 and Table 2). A colour fading was observed in the films (Fig. 1 A, upper part) as the photo-crosslinking time increased, and the films became almost colourless after 2 h. These colour changes were quantified by measuring the colour parameters (Fig. 1 B) as well as the Vis-light absorbance capacity of films (Fig. 1 C). The results indicated that L* remained unchanged, which was related to the insignificant variations in transparency values (Table 2), as also observed by Taghizadeh and colleagues (Taghizadeh et al., 2018) on photo-crosslinked riboflavin-containing gelatin films. Colour measurements also showed that a* increased (toward redness) while b* decreased (towards blueness). This led to perceptible colour differences ($\Delta E^* > 2$) (Nkhata, 2020), which became more noticeable as photo-crosslinking time increased. Besides, a hypochromic effect (intensity reduction) between 400 and 500 nm (λ_{max} at 450 nm, colour absorbed violet, colour seen yellow) was seen in the films (Fig. 1 C), which was also related to yellow colour fading in the films. In addition to changes in the Vis region, absorbance variations in the UV region (200–380 nm) were also observed as photo-crosslinking time increased: a shifting and absorbance increase of the band at 270 nm as well as absorbance increase between 310 and 320 nm and the disappearance of the band with λ_{max} at 366 nm. Considering that riboflavin has an absorption peak at around 445 nm in the Vis region, and three peaks around 375, 265 and 220 nm in the UV region, the absorbance changes in the films could be related to the partaking of riboflavin in the cross-linking reaction with gelatin (Kim, Kim, Song, Kang, & Park, 2020; Lee et al., 2023).

To better understand the photo-crosslinking process of gelatin films, the structures of gelatin films were assessed using FTIR and XRD techniques. The FTIR analysis of individual components can be found in the supplementary data (Fig. S2). In the analysis of films (Fig. 1 E, Table 2, Table S1 - Positions of the FTIR bands for films), small shifts of the Amide II band were observed as the photo-crosslinking time increased. Alterations in FTIR bands have been related to structural changes that occurred during the photo-crosslinking reaction between gelatin and riboflavin, which indicated that riboflavin-mediated UV irradiation-induced cross-linking in the presence of proteins (Wang, K. et al., 2017). Regarding the XRD outcomes (Fig. 1 F), the results showed that non-photo-crosslinked films (t0, control1) displayed two diffraction peaks: a small shoulder at 7.5°, assigned to the triple-helix structure, and a broad band at 20°, related to the partial crystalline structure of gelatin (Díaz-Calderon et al., 2017; Morsy, Hosny, Reicha, & Elnimr, 2017; Sahraee, Ghanbarzadeh, Milani, & Hamishehkar, 2017). Some changes could be observed due to the photo-crosslinking since the shoulder at 7.5° almost disappeared as compared to non-photo-crosslinked (t0) films. These changes indicated that the triple-helix structure development during film formation was hindered due to the photo-crosslinking reaction. Whittaker and colleagues (Whittaker, Choudhury, Dutta, & Zannettino, 2014) also observed changes in silk fibroin films to more amorphous structures when the protein was photo-crosslinked using tris (2,2′-bipyridyl)dichlororuthenium(II) and ammonium.

The formation of crosslinks between gelatin and riboflavin was indirectly measured via solubility assessment (Table 2). After 1 h of photo-crosslinking, films remained soluble in water, indicating that there was no formation of crosslinks or that the formed ones were not strong enough and stable to make films insoluble. As the photo-crosslinking time increased up to 2 h, the solubility reduced by 71%. Similar results were found by Wang and colleagues (Wang, K. et al., 2017), who explained that the decrease in the solubility of films was due to the formation of a highly crosslinked system. In fact, under UV or Vis light radiation, riboflavin absorbs light energy to create radical active oxygen species that promote crosslinking in the polymer, for example,

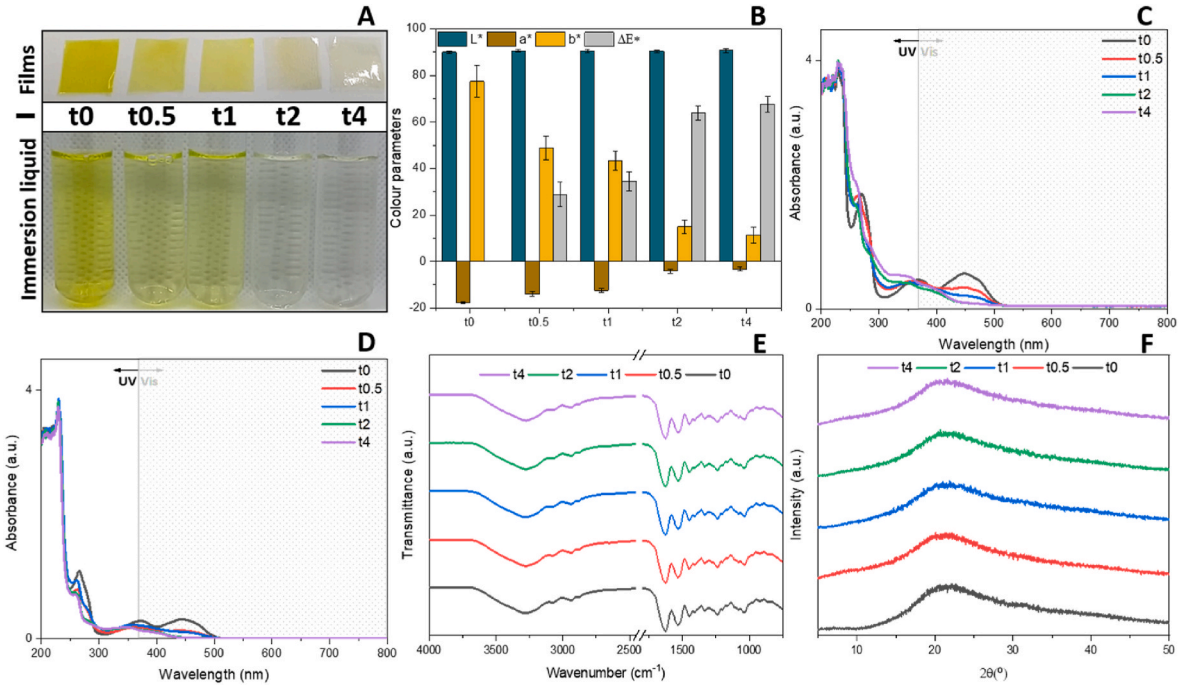

Fig. 1. A) Photo of the films (up) and the liquid after film immersion in water (down), **B)** colour parameters of films, UV–vis spectra of **C)** films and **D)** the immersion liquid, **E)** FTIR spectra and **F)** XRD patterns of gelatin films photo-crosslinked with riboflavin as a function of photo-crosslinking time (0, 0.5, 1, 2, and 4 h).

Table 2
Transparency, Amide II band position, and solubility of gelatin films photo-crosslinked with riboflavin as a function of photo-crosslinking time (0, 0.5, 1, 2, and 4 h). Means that do not share a letter in the same column are significantly ($p < 0.05$) different.

Film	Transparency	Amide II (cm^{-1})	Solubility (%)
t0	0.48 ± 0.03^{a}	1533.3 ± 0.6^{a}	100^{a}
t0.5	0.52 ± 0.05^{a}	1532.0 ± 0.0^{ab}	100^{a}
t1	0.54 ± 0.06^{a}	1531.3 ± 0.6^{b}	100^{a}
t2	0.49 ± 0.05^{a}	1531.3 ± 0.6^{b}	30.17 ± 1.94^{b}
t4	0.42 ± 0.04^{a}	1531.7 ± 0.6^{b}	28.66 ± 1.50^{b}

via covalent bond generation with the amine groups in proteins (Lee et al., 2023; Tirella, Liberto, & Ahluwalia, 2012; Wang, K. et al., 2017). As observed in Table 2, longer crosslinking times (up to 4 h) did not induce significant solubility variation. Taghizadeh and co-workers (Taghizadeh et al., 2018) also employed different UV exposure times (2, 4 and 6 h) to crosslink gelatin films. They observed that the greatest solubility reduction was obtained for 4 h-UV-treated gelatin films containing 25% glycerol.

The soluble part of the films (~29%) could be related to the uncrosslinked gelatin and riboflavin, as observed via UV–Vis absorption (Fig. 1 D) of the immersion liquid (Fig. 1 A, bottom part). Gelatin absorbs in the UV region from 200 to 300 nm due to the presence of peptide bonds and chromophores, while riboflavin absorbs in both the UV and Vis regions, as indicated above. As can be seen in Fig. 1 A (bottom part), immersion liquid became colourless as the photo-crosslinking time increased. This was due to more amount of the crosslinker taking part in the photo-crosslinking reaction and so, there was less riboflavin to be released in the water. In addition to these compounds, glycerol (10 wt %) could also be present in the soluble part due to its high hydrophilicity and low molecular weight (Taghizadeh et al., 2018; Wang, K. et al., 2017).

The changes in the structures of the films along with the colour and solubility test outcomes showed that gelatin was photo-crosslinked in the presence of riboflavin and a minimum of 2 h of light exposure. All in all, the photo-crosslinking time of 2 h was chosen as an optimal time to photo-crosslink the gelatin films with riboflavin. This selection was done based on the results obtained: films became almost colourless, the solubility dropped down to 30% and almost no riboflavin was dissolved in water after 2 h of photo-crosslinking.

3.2. Selection of CNWs type and concentration

The addition of CNWs affected the colour of the films (Fig. 2 A): L* remained unchanged (so did the transparency, Table 3), a* slightly increased while b* decreased. Wang and colleagues (Wang, L., Shankar, & Rhim, 2017) also observed variations in a* and b* parameters while L* remained unchanged in alginate-based films reinforced with cellulose fibres and cellulose nanowhiskers. Regarding the UV–Vis absorbance capacity of films, no differences could be observed as CNWs were added, regardless of their type and concentration (Fig. 2 B). Haghighi and co-authors (Haghighi et al., 2021) also observed that the addition of bacterial cellulose nanowhiskers (up to 10%) did not affect the UV–Vis transmittance of gelatin/polyvinyl alcohol films. The authors suggested that the nanowhiskers were dispersed uniformly and so, there were no UV–Vis light absorption nor transparency changes in the films.

The analysis of the secondary structure of the films using FTIR showed that the Amide A band slightly shifted to lower wavenumbers (Table 3 and Table S2 - Positions of the FTIR bands for films) and its intensity increased (Fig. 2 C), compared to t2 films (2 h-photo-crosslinked films without CNWs, control2), when CNWs were added. These outcomes could be mainly related to H-bonding between the alcohol (–OH) groups of CNWs and the amine ($–NH_2$) groups of gelatin (Fig. S3) (Wang, L. et al., 2017). The outcomes confirmed that increasing the AH-CNWs concentration from 2 to 4 wt % promoted more interactions, while the increase in TEMPO-CNWs concentration did not.

As for the crystalline structure of gelatin films, first, the CNWs and the effect of UV exposure on the crystalline properties of the nanostructures were assessed (Fig. 2 D). The crystal structure of CNWs was confirmed by the presence of very intense peaks at around 9° and 19° (Nguyen, de Vries, & Stoyanov, 2022). It was also observed that, unlike AH-CNWs, the intensity of the crystalline peak at 19° of the TEMPO-CNWs powder decreased after 2 h of UV–Vis light exposure,

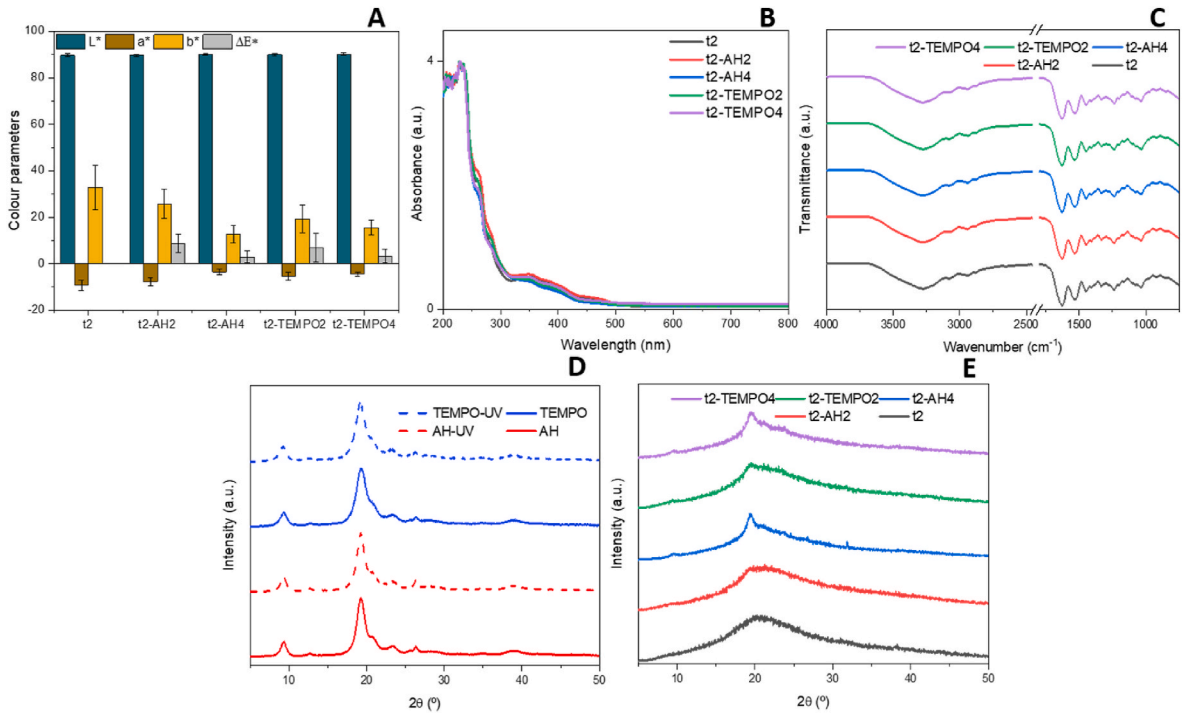

Fig. 2. **A)** Colour parameters, **B)** UV–vis spectra, **C)** FTIR spectra and **E)** XRD patterns of gelatin films photo-crosslinked with riboflavin as a function of CNWs type (AH and TEMPO) and their contents (2 and 4 wt %). **D)** XRD patterns of AH and TEMPO CNWs powders as a function of UV-light exposure: AH and TEMPO (no UV exposure) and AH-UV and TEMPO-UV (2 h of UV exposure).

Table 3
Transparency, Amide A band position and solubility of gelatin films photo-crosslinked with riboflavin for 2 h, as a function of CNWs type (AH and TEMPO) and their contents (2 and 4 wt %). Means that do not share a letter in the same column are significantly ($p < 0.05$) different.

Film	Transparency	Amide A (cm^{-1})	Solubility (%)
t2	0.44 ± 0.04^{a}	3279.3 ± 0.6^{a}	30.17 ± 1.94^{a}
t2-AH2	0.53 ± 0.07^{a}	3274.3 ± 4.9^{ab}	29.82 ± 3.87^{a}
t2-AH4	0.48 ± 0.07^{a}	3271.3 ± 0.6^{b}	24.15 ± 2.82^{b}
t2-TEMPO2	0.40 ± 0.02^{a}	3271.0 ± 1.0^{b}	21.80 ± 1.90^{b}
t2-TEMPO4	0.45 ± 0.06^{a}	3272.0 ± 0.0^{b}	24.01 ± 2.30^{b}

which could be directly linked to both a decrease in crystallinity in the CNW and the differences observed in FTIR results (presence/lack of interactions with gelatin, Fig. 2 C and Table 3). Similar results were observed in the literature (Zia, Barikani, Bhatti, Zuber, & Barmar, 2009). Regarding the films, the addition of CNWs induced changes in the XRD diffraction patterns of the samples (Fig. 2 E). New peaks at around 9° and 19° were seen, indicating the presence of highly crystalline structure of CNWs (Fig. 2 D) (Nguyen et al., 2022). The intensity and narrowness of the 19° peak were more pronounced with the increase in CNW content, especially with AH-CNWs. These different behaviours in the crystallinity of the CNWs used in this study could be related to their photo-stability after light exposure (Fig. 2 D).

Regarding the effect of CNWs on the solubility of the films, an increase in water stability with the addition of CNWs was observed (Table 3). This solubility reduction was related to the presence of interactions such as H-bonds, as observed via FTIR analysis (Fig. 2 C and Table 3), as well as the presence of non-water soluble and crystalline nanocomponents (the CNWs themselves) in the film (Jamróz, Kulawik, & Kopel, 2019). All this provided films with better water stability.

It has been shown that the inclusion of nanostructures (sizes lying in the range of 100 nm) into the biopolymer matrices as reinforcing fillers markedly changes the mechanical properties of the final nanocomposite materials (Marangoni Júnior, Rodrigues, Silva, Vieira, & Alves, 2022). Therefore, the mechanical properties of CNW-containing gelatin films were assessed and the results are shown in Table 4. The addition of CNWs notably increased the E and TS values of films while EB values decreased, compared to t2 (control2), and the effect was greater as their concentration increased. Similar results were seen in cellulose nanowhiskers reinforced chitosan and alginate films (Rong, Mubarak, & Tanjung, 2017; Wang, L. et al., 2017). These alterations could be related to the formation of interactions between gelatin and CNWs, as seen via FTIR (Fig. 2 C) as well as the crystalline nature of the nanocompounds (Fig. 2 D and E).

On the whole, the AH-CNW at 4 wt % was chosen as the optimal CNW type and concentration due to its photostability as well as its effect on the solubility and mechanical properties of films. In these latter properties, the t2-AH4 films presented E, TS and EB values which are within the range values of commercially available synthetic packaging films (Bastarrachea, Dhawan, & Sablani, 2011; Mangaraj, Goswami, & Mahajan, 2009).

3.3. *Nisin A®concentration selection*

The addition of Nisin A® did not have significant effects on a*, while L* slightly decreased (so did the transparency, Table 5) and b* increased (Fig. 3 A). These alterations in colour parameters resulted in predictable

Table 4
Elastic modulus (E), tensile strength (TS) and elongation at break (EB) of gelatin films photo-crosslinked with riboflavin for 2 h, as a function of CNWs type (AH and TEMPO) and their contents (2 and 4 wt %). Means that do not share a letter in the same column are significantly ($p < 0.05$) different.

Film	E (MPa)	TS (MPa)	EB (%)
t2	146.6 ± 16.12^{a}	6.32 ± 0.42^{a}	93.0 ± 7.6^{a}
t2-AH2	262.7 ± 44.73^{b}	7.49 ± 0.54^{bc}	78.2 ± 4.5^{b}
t2-AH4	400.2 ± 33.01^{c}	8.15 ± 0.35^{c}	44.5 ± 7.3^{cd}
t2-TEMPO2	261.5 ± 47.51^{b}	7.45 ± 0.65^{bc}	56.5 ± 5.7^{c}
t2-TEMPO4	350.5 ± 69.72^{c}	6.80 ± 0.28^{ab}	35.6 ± 6.7^{c}

Table 5
Transparency, water vapour permeability (WVP) and solubility values for gelatin films photo-crosslinked with riboflavin for 2 h and containing 4 wt % AH-CNWs, as a function of Nisin A® content (0, 7.5, 15 and 30 wt%). Means that do not share a letter in the same column are significantly ($p < 0.05$) different.

Film	Transparency	WVP ˆ12 (g/(cm·s·Pa))	Solubility (%)
t2-AH4	0.59 ± 0.17^{a}	2.5 ± 0.5	24.15 ± 2.82^{a}
t2-AH4-Ni7.5	0.58 ± 0.15^{a}	2.3 ± 0.6	25.78 ± 3.17^{a}
t2-AH4-Ni15	2.10 ± 0.42^{b}	3.3 ± 0.5	33.94 ± 5.21^{b}
t2-AH4-Ni30	2.17 ± 0.46^{b}	3.9 ± 0.2	37.96 ± 1.95^{b}

colour differences which became more noticeable as Nisin A® concentration increased. Similar results were also observed by Leelaphiwat and colleagues (Leelaphiwat, Pechprankan, Siripho, Bumbudsanpharoke, & Harnkarnsujarit, 2022) in poly(butylene adipate terephthalate) and thermoplastic starch blends films. The authors observed that as nisin content increased the yellowish colour of the films also increased. In the current study, colour changes were related to the slightly yellowish colour of the employed Nisin A® powder. Changes were also observed in the UV–Vis light absorbance capacity of films, especially in 15 and 30 wt % Nisin A®-containing films (Fig. 3 B). This could be related to the presence of some unsaturated double bonds conjugated to saturated covalent bonds in nisin (Luciano et al., 2021) but mainly to the light scattering and reflecting aroused from the non-pure Nisin A® product (Qi et al., 2022). It is worth mentioning that the films had excellent UV light barrier properties which can be considered a preventive (secondary) antioxidant function in active packaging. This protection from light may lower the occurrence of photo-oxidation reactions in foods (Etxabide et al., 2022).

As for the secondary structure of gelatin (Fig. 3 C and Table S3), the addition of Nisin A® did not induce any shifts in the main bands of gelatin which was interpreted as the lack of new interactions between the Nisin A® components (NaCl and nisin -a peptide-itself) and the other components of the formulation. This unbounded property of Nisin A® could facilitate the release of the antimicrobial agent from the films into the food, an interesting property for active packaging applications, which is studied later on.

The previously observed crystalline structure of films (Fig. 2 D) showed notable differences when the antimicrobial agent was added, as seen in the XRD results (Fig. 3 D). The addition of Nisin A® reduced the crystallinity of gelatin as seen via the broadening and intensity reduction of the peaks at 2θ values of 7.5° and 20°. Similar results were observed in nisin-containing starch nanocomposite films (Meira, Zehetmeyer, Werner, & Brandelli, 2017). The authors observed that the XRD spectrum of nisin showed no remarkable peaks, indicating a predominantly amorphous behaviour. When nisin was incorporated into the film formulation, the helical formation of amylose complexes was hindered, and so the crystallinity decreased since peaks became broader and almost disappeared. Therefore, in the current study, the addition of Nisin A® also led to more amorphous structures.

Due to the composition of Nisin A® employed in this work (2.1 Materials section), NaCl crystals were present in the films, as seen by XRD peaks at $2\theta = 27.5°$, 31.7°, 45.5° (Fig. 3 D) and SEM image (Fig. 3 E). A similar observation was made by Qi and colleagues (Qi et al., 2022) on nisin-containing ethylene vinyl alcohol films which presented a strong peak at $2\theta = 31.5°$ associated with the characteristic diffraction of NaCl. The high content of NaCl in the films developed in the current study could be responsible for the transparency reduction (light scattering and reflecting), which could be observed in the UV–Vis spectrum of the studied gelatin films (Fig. 3 B).

Further morphological characterizations (Fig. 4) showed that as the Nisin A® concentration increased, rougher cross-sections of films were obtained, compared to the control films (without Nisin A®, Fig. 4 A). This could be related to the partial aggregation of nisin, as observed by Zehetmeye and colleagues (Zehetmeyer et al., 2016) on nisin-containing poly(butylene adipate-co-terephthalate) films, but mainly because of the high presence of NaCl in the antimicrobial compound (nisin or pediocin), as seen by Meira and co-authors on antimicrobial peptides-containing starch-halloysite films (Meira et al., 2017).

It is well known that changes in morphology and chemical composition can affect the barrier and mechanical properties of (bio)polymers and so, the water vapour permeability and mechanical behaviour of the

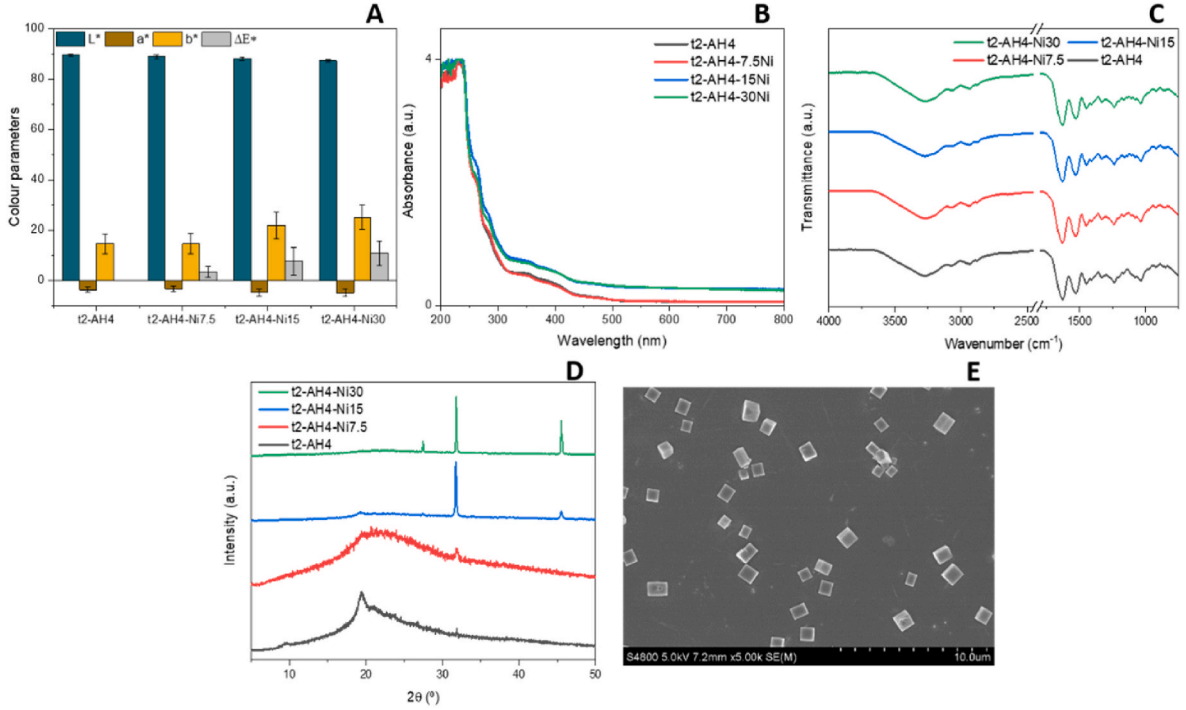

Fig. 3. **A)** Colour parameters, **B)** UV–vis spectra, **C)** FTIR spectra and **D)** XRD patterns of gelatin films photo-crosslinked with riboflavin for 2 h and containing 4 wt % AH-CNWs, as a function Nisin A® content (0, 7.5, 15 and 30 wt %). **E)** SEM images of t2-AH4-Ni15.

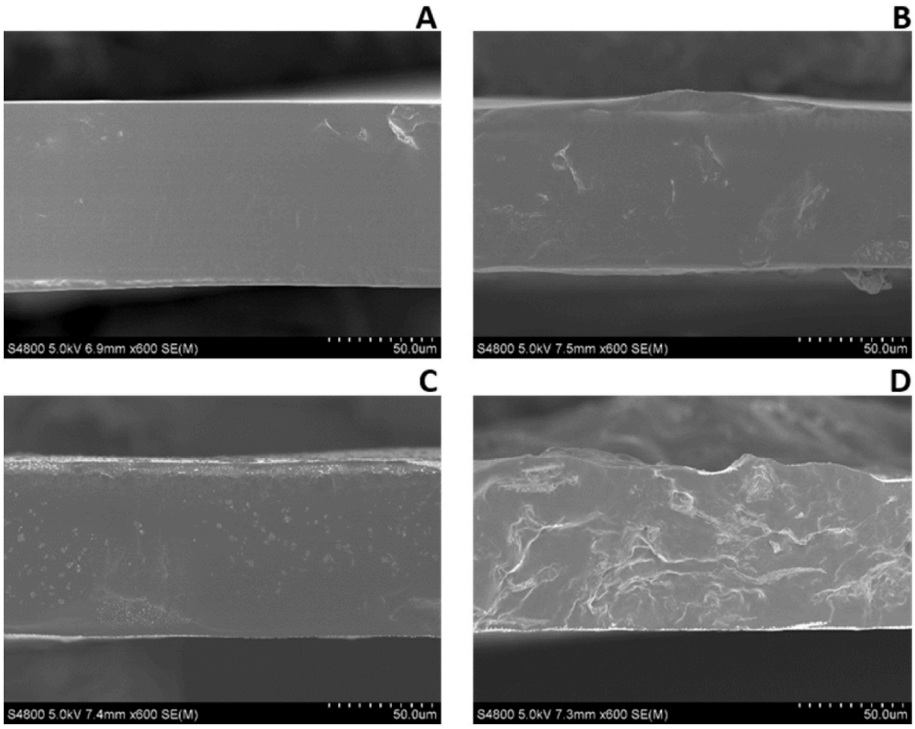

Fig. 4. SEM images of gelatin films photo-crosslinked with riboflavin for 2 h and containing 4 wt % AH-CNWs, as a function of Nisin A® content: A) 0, B) 7.5, C) 15 and D) 30 wt %.

films were assessed (Tables 5 and 6). It was seen that the addition of Nisin A® slightly increased the WVP values of the gelatin film (Table 5). The same trend was observed in nisin-containing gelatin and ethylene vinyl alcohol films, where the changes in WVP could be related to the loosen matrix effect of nisin (Luciano et al., 2021; Qi et al., 2022) as also seen in our study (Fig. 3 D), as well as the strong affinity to the water of both nisin and NaCl. As for the mechanical properties of the films (Table 6), the addition of Nisin A® notably decreased the E and TS values of films while EB values increased, compared to t2-AH4 (control3). These alterations could be related to a reduction in the crystallinity of gelatin (Fig. 2 D) as well as to the hygroscopy nature of nisin and NaCl which made films more flexible.

Regarding the behaviour of the films when in contact with water, it was observed that the solubility of films increased with the Nisin A® addition (Table 5). Similar behaviour was observed in nisin-containing starch/hydroxypropyl methylcellulose and gelatin films (Basch, Jagus, & Flores, 2013; Luciano et al., 2021). Luciano and colleagues related the increase in film solubility as nisin content increased with the reduction observed for the $2\theta = 7°$ peak, also observed in the current study. As interactions between the Nisin A® and the other components of the formulation were not observed in the present study (Fig. 3 C), the increase in solubility could mainly be related to the presence of unbounded Nisin A® (both NaCl and nisin), which could be released in higher quantities when present in higher amounts in films (Fig. S4) and, in turn, increased film solubility. The release of Nisin A® from the film into a food simulant showed that these films could be of interest for active packing applications.

The antimicrobial activity of the films was studied over both the native microbiota from various food myosystems and specific pathogen (or their subrogates) or spoilage strains from culture collection. As shown in Table 7, t2-AH4 film (without Nisin A®, control3) had no antimicrobial activity, despite the presence of riboflavin in the

Table 6
Elastic modulus (E), tensile strength (TS) and elongation at break (EB) of gelatin films photo-crosslinked with riboflavin for 2 h and containing 4 wt % AH-CNWs, as a function of Nisin A® content (0, 7.5, 15 and 30 wt %). Means that do not share a letter in the same column are significantly ($p < 0.05$) different.

Film	E (MPa)	TS (MPa)	EB (%)
t2-AH4	400.20 ± 33.01[a]	8.15 ± 0.35[a]	44.50 ± 7.30[a]
t2-AH4-Ni7.5	41.20 ± 1.81[b]	1.56 ± 0.07[b]	90.93 ± 4.11[b]
t2-AH4-Ni15	54.82 ± 19.21[b]	0.42 ± 0.07[b]	101.08 ± 15.27[b]
t2-AH4-Ni30	72.94 ± 21.22[b]	0.85 ± 0.17[b]	112.26 ± 5.47[b]

Table 7
Antimicrobial activity expressed as inhibition halos (mm) over different strains and food homogenates of gelatin films photo-crosslinked with riboflavin for 2 h and containing 4 wt % AH-CNWs, as a function of Nisin A® content (0, 7.5, 15 and 30 wt %). Dahses (–) indicate no antimicrobial activity. Means that do not share a capital letter in the same row are significantly ($p < 0.05$) different. Means that do not share a lowercase letter in the same column are significantly ($p < 0.05$) different.

Strains	Antimicrobial activity of films (inhibition halo, in mm)			
	t2-AH4	t2-AH4-Ni7.5	t2-AH4-Ni15	t2-AH4-Ni30
E. coli K12	–	13.0 ± 0.0Aa	13.2 ± 0.2Aa	14.0 ± 1.4Aa
B. cereus	–	–	–	–
B. termosphacta	–	13.0 ± 0.0Aa	14.5 ± 0.3Bb	14.7 ± 1.1Ba
P. fluorescens	–	14.0 ± 0.1Ab	–	14.1 ± 0.0Aa
A. hydrophila	–	–	–	13.7 ± 0.6a
P. phosphoreum	–	–	–	–
Food native microbiota	**t2-AH4**	**t2-AH4-Ni7.5**	**t2-AH4-Ni15**	**t2-AH4-Ni30**
Chicken breast fillets	–	13.7 ± 0.6Aa	16.1 ± 0.9Ba	14.8 ± 0.5Ba
Sliced cold-smoked salmon	–	14.3 ± 0.0Aa	–	14.5 ± 0.0Ba
Minced beef meat	–	–	–	–
Sea bream fillet	–	14.8 ± 0.9Aa	14.0 ± 1.3Aa	15.0 ± 1.2Aa

formulation. Riboflavin has been recently suggested as a promising antimicrobial compound (Farah et al., 2022), however, its partaking in the crosslinking reaction with gelatin (Fig. 1) could be a reason for not showing any active properties. On the contrary, Nisin A® addition to the film formulation showed antimicrobial activity, regardless of its concentration, in most of the tested strains as well as native microbiota from chilled cold-smoked salmon, breast chicken fillets and sea bream fillets. The antimicrobial activity was mainly circumscribed to the film's contact area (13 mm) and, in some cases, it was slightly higher when higher Nisin A® concentrations (15 and 30 wt %) were used. This result is not surprising, as the inhibition halo is dependent on diffusion through the agar media, due to the non-volatility of Nisin A®. In any case, the presence of a greater inhibition halo should be interpreted as a stronger antimicrobial effect. It should be highlighted that *B. cereus, P. phosphoreum*, and the native microbiota of chilled minced beef meat were not inhibited by any film.

The Nisin A® used in this study contains two main components: NaCl and nisin. As for the salt (NaCl), it has no specific antimicrobial action but develops a general bacteriostatic effect, retarding microbial growth to a greater or lesser extent depending on the concentration used. At sufficiently high concentrations, the salt produces an osmotic imbalance in the microbial cells, leading to shrinkage and reduction of cytoplasmic volume due to loss of water. Regarding the mode of action of nisin, its adsorption on the cell surface causes the disintegration of the cytoplasmic membrane structure. This is because its positive charge acts against the negative charge of the phospholipid layer of the bacterial cytoplasmic membrane. So, the nature and content of the cell membrane phospholipids play an important role in determining bacterial sensitivity to nisin (Eghbal, Chihibn, & Gharsallaoui, 2020). Generally, it is described that Gram-positive bacteria are highly sensitive to nisin, even the sporulated forms (Eghbal et al., 2020). So, it is surprising the observed resistance of *B. cereus*, which may be attributed to the specific strain used. Regarding the antimicrobial activity of films on minced beef, it has previously been reported nisin's antimicrobial activity on meat and meat products (Eghbal et al., 2020; Garavito, Moncayo-Martínez, & Castellanos, 2020). It has also been described that nisin may exert a weaker antimicrobial activity in meat than when assayed *in vitro* over microbial strains (Cutter & Siragusa, 1995a, 1995b; Eghbal et al., 2020). Possible explanations are interaction with phospholipids, low solubility and partial inactivation by endogenous meat enzymes (Figueiredo & Almeida, 2017). These effects were not observed in the other studied myosystems, since good antimicrobial activity was obtained in fresh sea bream, cold-smoked salmon and chicken breast fillets. Indeed, many reports can be found on the antimicrobial activity of nisin in these food products (Eghbal et al., 2020; Garavito et al., 2020).

4. Conclusions

In this study, antimicrobial gelatin films with improved physicochemical properties were prepared via the solution casting technique with the main aim of providing food safety as well as extending the shelf life of packaged foods and, in turn, helping reduce food waste via food spoilage reduction. For that, a combined strategy of photo-crosslinking with riboflavin and compounding with different types and concentrations of chitin nanowhiskers was employed and the optimized conditions were 2 h of photo-crosslinking time and compounding with 4 wt % of acid hydrolysis-produced chitin nanowhiskers. The films showed low water solubility (~24%) and mechanical properties similar to those of conventional packaging materials. Finally, the commercial antimicrobial compound Nisin A® was incorporated into the films at different concentrations. These films showed excellent UV light barrier properties (prevent photo-oxidation) and good antibacterial properties over some selected pathogen or spoilage strains, as well as native microbiota of chilled sea bream fillets, cold-smoked salmon and chicken breast fillets due to the composition of Nisin A® (nisin + NaCl) incorporated in the film formulation. Therefore, the films developed in this study could be promising candidates for extending the shelf life of these kinds of food products and preventing food waste.

CRediT author statement

Alaitz Etxabide: Conceptualization, Methodology, Formal analysis, Investigation, Writing - Original Draft, Funding acquisition; Daniel Mojío: Formal analysis, Investigation; Pedro Guerrero: Methodology, Writing - Review & Editing; Koro de la Caba: Resources, Writing - Review & Editing; Joaquín Gómez-Estaca: Conceptualization, Investigation, Resources, Writing - Review & Editing, Supervision, Funding acquisition.

Declaration of competing interest

The authors declare that they have no known competing financial interests or personal relationships that could have appeared to influence the work reported in this paper.

Data availability

No data was used for the research described in the article.

Acknowledgement

The authors would like to thank the Spanish Ministry of Science and Innovation (projects PID2019-108361RB-I00 and AGL2017-84161-C2-1-R) for funding. A.E. thanks the State Research Agency of Spain within the Juan de la Cierva - Incorporation action (IJC2019-039697I). The authors also thank the Basque Government for funding through the research groups of the Basque University System (IT1658-22) and the Consejo Superior de Investigaciones Científicas-CSIC (project 245025).

Appendix A. Supplementary data

Supplementary data to this article can be found online at https://doi.org/10.1016/j.foodhyd.2023.109371.

References

ASTM D882-02. (2002). *Standard test method for tensile properties of thin plastic sheeting*. https://www.astm.org/d0882-02.html.

ASTM E96-00. (2000). *Standard test methods for water vapor transmission of materials*. https://www.astm.org/e0096-00.html.

Bahrami, A., Delshadi, R., Jafari, S. M., & Williams, L. (2019). Nanoencapsulated nisin: An engineered natural antimicrobial system for the food industry. *Trends in Food Science and Technology, 94*, 20–31. https://doi.org/10.1016/j.tifs.2019.10.002

Basch, C. Y., Jagus, R. J., & Flores, S. K. (2013). Physical and antimicrobial properties of tapioca starch-HPMC edible films incorporated with nisin and/or potassium sorbate. *Food and Bioprocess Technology, 6*, 2419–2428. https://doi.org/10.1007/s11947-012-0860-3

Bastarrachea, L., Dhawan, S., & Sablani, S. S. (2011). Engineering properties of polymeric-based antimicrobial films for food packaging: A review. *Food Engineering Reviews, 3*, 79–93. https://doi.org/10.1007/s12393-011-9034-8

Cutter, C. N., & Siragusa, G. R. (1995a). Treatments with nisin and chelators to reduce salmonella and escherichia coli on beef. *Journal of Food Protection, 58*, 1028–1030. https://doi.org/10.4315/0362-028X-58.9.1028

Cutter, C. N., & Siragusa, G. R. (1995b). Population reductions of gram-negative pathogens following treatments with nisin and chelators under various conditions. *Journal of Food Protection, 58*, 977–983. https://doi.org/10.4315/0362-028X-58.9.977

Díaz-Calderón, P., Flores, E., González-Muñoz, A., Pepczynska, M., Quero, F., & Enrione, J. (2017). Influence of extraction variables on the structure and physical properties of salmon gelatin. *Food Hydrocolloids, 71*, 118–128. https://doi.org/10.1016/j.foodhyd.2017.05.004

Eghbal, N., Chihibn, O. E., & Gharsallaoui, A. (2020). Nisin. In P. M. Davidson, T. M. Taylor, & J. R. D. David (Eds.), *Antimicrobials in food*. CRC Press.

Etxabide, A., Garrido, T., Uranga, J., Guerrero, P., & de la Caba, K. (2018). Extraction and incorporation of bioactives into protein formulations for food and biomedical applications. *International Journal of Biological Macromolecules, 120*, 2094–2105. https://doi.org/10.1016/j.ijbiomac.2018.09.030

Etxabide, A., Kilmartin, P. A., Maté, J. I., & Gómez-Estaca, J. (2022). Characterization of glucose-crosslinked gelatin films reinforced with chitin nanowhiskers for active packaging development. *Lwt, 154*, Article 112833. https://doi.org/10.1016/j.lwt.2021.112833

European Commission. (2022). *Food loss and waste prevention*. https://food.ec.europa.eu/horizontal-topics/farm-fork-strategy/food-loss-and-waste-prevention_en.

Fadiji, T., Rashvand, M., Daramola, M. O., & Iwarere, S. A. (2023). A review on antimicrobial packaging for extending the shelf life of food. *Processes, 11*, 590. https://doi.org/10.3390/pr11020590

Fael, H., & Demirel, A. L. (2020). Nisin/polyanion layer-by-layer films exhibiting different mechanisms in antimicrobial efficacy. *RSC Advances, 10*, 10329–10337. https://doi.org/10.1039/C9RA10135G

Fan, Y., Saito, T., & Isogai, A. (2008). Chitin nanocrystals prepared by TEMPO-mediated oxidation of α-chitin. *Biomacromolecules, 9*, 192–198. https://doi.org/10.1021/bm700966g

Farah, N., Chin, V. K., Chong, P. P., Lim, W. F., Lim, C. W., Basir, R., et al. (2022). Riboflavin as a promising antimicrobial agent? A multi-perspective review. *Current Research in Microbial Sciences, 3*, Article 100111. https://doi.org/10.1016/j.crmicr.2022.100111

Figueiredo, A. C. L., & Almeida, R. C. C. (2017). Antibacterial efficacy of nisin, bacteriophage P100 and sodium lactate against listeria monocytogenes in ready-to-eat sliced pork ham. *Brazilian Journal of Microbiology, 48*, 724–729. https://doi.org/10.1016/j.bjm.2017.02.010

Garavand, F., Rouhi, M., Razavi, S. H., Cacciotti, I., & Mohammadi, R. (2017). Improving the integrity of natural biopolymer films used in food packaging by crosslinking approach: A review. *International Journal of Biological Macromolecules, 104*, 687–707. https://doi.org/10.1016/j.ijbiomac.2017.06.093

Garavito, J., Moncayo-Martínez, D., & Castellanos, D. A. (2020). Evaluation of antimicrobial coatings on preservation and shelf life of fresh chicken breast fillets under cold storage. *Foods, 9*, 1203. https://doi.org/10.3390/foods9091203

Haghighi, H., Gullo, M., La China, S., Pfeifer, F., Siesler, H. W., Licciardello, F., et al. (2021). Characterization of bio-nanocomposite films based on gelatin/polyvinyl alcohol blend reinforced with bacterial cellulose nanowhiskers for food packaging applications. *Food Hydrocolloids, 113*, Article 106454. https://doi.org/10.1016/j.foodhyd.2020.106454

Holcapkova, P., Raskova, Z. K., Hrabalikova, M., Salakova, A., Drbohlav, J., & Sedlarik, V. (2017). Isolation and thermal stabilization of bacteriocin nisin derived from whey for antimicrobial modifications of polymers. *International Journal of Polymer Science, 2017*. https://doi.org/10.1155/2017/3072582, 0-7.

Hosseini, S. F., & Gómez-Guillén, M. C. (2018). A state-of-the-art review on the elaboration of fish gelatin as bioactive packaging: Special emphasis on nanotechnology-based approaches. *Trends in Food Science & Technology, 79*, 125–135. https://doi.org/10.1016/j.tifs.2018.07.022

Jamróz, E., Kulawik, P., & Kopel, P. (2019). The effect of nanofillers on the functional properties of biopolymer-based films: A review. *Polymers, 11*, 675. https://doi.org/10.3390/polym11040675

Kim, E., Kim, M. H., Song, J. H., Kang, C., & Park, W. H. (2020). Dual crosslinked alginate hydrogels by riboflavin as photoinitiator. *International Journal of Biological Macromolecules, 154*, 989–998. https://doi.org/10.1016/j.ijbiomac.2020.03.134

Leelaphiwat, P., Pechprankan, C., Siripho, P., Bumbudsanpharoke, N., & Harnkarnsujarit, N. (2022). Effects of nisin and EDTA on morphology and properties of thermoplastic starch and PBAT biodegradable films for meat packaging. *Food Chemistry, 369*, Article 130956. https://doi.org/10.1016/j.foodchem.2021.130956

Lee, Y. B., Lim, S., Lee, Y., Park, C. H., & Lee, H. J. (2023). Green chemistry for crosslinking biopolymers: Recent advances in riboflavin-mediated photochemistry. *Materials, 16*, 1218. https://doi.org/10.3390/ma16031218

Liao, J., Zhou, Y., Hou, B., Zhang, J., & Huang, H. (2023). Nano-chitin: Preparation strategies and food biopolymer film reinforcement and applications. *Carbohydrate Polymers, 305*, Article 120553. https://doi.org/10.1016/j.carbpol.2023.120553

Li, C., Sheng, L., Sun, G., & Wang, L. (2020). The application of ultraviolet-induced photo-crosslinking in edible film preparation and its implication in food safety. *Lwt, 131*, Article 109791. https://doi.org/10.1016/j.lwt.2020.109791

López-Carballo, G., Gómez-Estaca, J., Catalá, R., Hernández-Muñoz, P., & Gavara, R. (2012). 3 - active antimicrobial food and beverage packaging. In K. L. Yam, & D. S. Lee (Eds.), *Emerging food packaging technologies* (pp. 27–54). Woodhead Publishing.

Luciano, C. G., Tessaro, L., Lourenço, R. V., Bittante, A. M. Q. B., Fernandes, A. M., Moraes, I. C. F., et al. (2021). Effects of nisin concentration on properties of gelatin film-forming solutions and their films. *International Journal of Food Science and Technology, 56*, 587–599. https://doi.org/10.1111/ijfs.14731

Mangaraj, S., Goswami, T. K., & Mahajan, P. V. (2009). Applications of plastic films for modified atmosphere packaging of fruits and vegetables: A review. *Food Engineering Reviews, 1*, 133–158. https://doi.org/10.1007/s12393-009-9007-3

Marangoni Júnior, L., Rodrigues, P. R., Silva, R. G.d., Vieira, R. P., & Alves, R. M. V. (2022). Improving the mechanical properties and thermal stability of sodium alginate/hydrolyzed collagen films through the incorporation of SiO2. *Current Research in Food Science, 5*, 96–101. https://doi.org/10.1016/j.crfs.2021.12.012

Meira, S. M. M., Zehetmeyer, G., Werner, J. O., & Brandelli, A. (2017). A novel active packaging material based on starch-halloysite nanocomposites incorporating antimicrobial peptides. *Food Hydrocolloids, 63*, 561–570. https://doi.org/10.1016/j.foodhyd.2016.10.013

Morsy, R., Hosny, M., Reicha, F., & Elnimr, T. (2017). Developing and physicochemical evaluation of cross-linked electrospun gelatin–glycerol nanofibrous membranes for medical applications. *Journal of Molecular Structure, 1135*, 222–227. https://doi.org/10.1016/j.molstruc.2017.01.064

Müller-Auffermann, K., Grijalva, F., Jacob, F., & Hutzler, M. (2015). Nisin and its usage in breweries: A review and discussion. *Journal of the Institute of Brewing, 121*, 309–319. https://doi.org/10.1002/jib.233

Nguyen, H. V. D., de Vries, R., & Stoyanov, S. D. (2022). Chitin nanowhiskers with improved properties obtained using natural deep eutectic solvent and mild mechanical processing. *Green Chemistry, 24*, 3834–3844. https://doi.org/10.1039/D2GC00305H

Nkhata, S. G. (2020). Total color change (ΔE*) is a poor estimator of total carotenoids lost during post-harvest storage of biofortified maize grains. *Heliyon, 6*, Article e05173. https://doi.org/10.1016/j.heliyon.2020.e05173

Packaging Europe. (2022). *How can active food packaging help us to avoid waste and improve food safety?*. https://packagingeurope.com/comment/how-can-active-food-packaging-help-us-to-avoid-waste-and-improve-food-safety/8284. article.

Popa, E. E., Miteluț, A. C., Râpă, M., Popescu, P. A., Drăghici, M. C., Geicu-Cristea, M., et al. (2022). Antimicrobial active packaging containing nisin for preservation of products of animal origin: An overview. *Foods, 11*, 3820. https://doi.org/10.3390/foods11233820

Qi, D., Xiao, Y., Xia, L., Li, L., Jiang, S., Jiang, S., et al. (2022). Colorimetric films incorporated with nisin and anthocyanins of pomegranate/clitoria ternatea for shrimp freshness monitoring and retaining. *Food Packaging and Shelf Life, 33*, Article 100898. https://doi.org/10.1016/j.fpsl.2022.100898

Rong, S. Y., Mubarak, N. M., & Tanjung, F. A. (2017). Structure-property relationship of cellulose nanowhiskers reinforced chitosan biocomposite films. *Journal of Environmental Chemical Engineering, 5*, 6132–6136. https://doi.org/10.1016/j.jece.2017.11.054

Sahraee, S., Ghanbarzadeh, B., Milani, J. M., & Hamishehkar, H. (2017). Development of gelatin bionanocomposite films containing chitin and ZnO nanoparticles. *Food and Bioprocess Technology, 10*, 1441–1453. https://doi.org/10.1007/s11947-017-1907-2

Soltani Firouz, M., Mohi-Alden, K., & Omid, M. (2021). A critical review on intelligent and active packaging in the food industry: Research and development. *Food Research International, 141*, Article 110113. https://doi.org/10.1016/j.foodres.2021.110113

Taghizadeh, M., Mohammadifar, M. A., Sadeghi, E., Rouhi, M., Mohammadi, R., Askari, F., et al. (2018). Photosensitizer-induced cross-linking: A novel approach for improvement of physicochemical and structural properties of gelatin edible films. *Food Research International, 112*, 90–97. https://doi.org/10.1016/j.foodres.2018.06.010

Tirella, A., Liberto, T., & Ahluwalia, A. (2012). Riboflavin and collagen: New crosslinking methods to tailor the stiffness of hydrogels. *Materials Letters, 74*, 58–61. https://doi.org/10.1016/j.matlet.2012.01.036

Vilela, C., Kurek, M., Hayouka, Z., Röcker, B., Yildirim, S., Antunes, M. D. C., et al. (2018). A concise guide to active agents for active food packaging. *Trends in Food Science & Technology, 80*, 212–222. https://doi.org/10.1016/j.tifs.2018.08.006

Wang, L., Shankar, S., & Rhim, J. (2017). Properties of alginate-based films reinforced with cellulose fibers and cellulose nanowhiskers isolated from mulberry pulp. *Food Hydrocolloids, 63*, 201–208. https://doi.org/10.1016/j.foodhyd.2016.08.041

Wang, K., Wang, W., Wu, X., Xiao, J., Liu, Y., & Liu, A. (2017). Effect of photochemical UV/riboflavin-mediated cross-links on different properties of fish gelatin films. *Journal of Food Process Engineering, 40*, Article e12536. https://doi.org/10.1111/jfpe.12536

Westlake, J. R., Tran, M. W., Jiang, Y., Zhang, X., Burrows, A. D., & Xie, M. (2023). Biodegradable biopolymers for active packaging: Demand, development and directions. *Sustainable Food Technology, 1*, 50–72. https://doi.org/10.1039/D2FB00004K

Whittaker, J. L., Choudhury, N. R., Dutta, N. K., & Zannettino, A. (2014). Facile and rapid ruthenium mediated photo-crosslinking of bombyx mori silk fibroin. *Journal of Materials Chemistry B, 2*, 6259–6270. https://doi.org/10.1039/C4TB00698D

Wong, N. G. K., Rhodes, C., & Dessent, C. E. H. (2021). Photodegradation of riboflavin under alkaline conditions: What can gas-phase photolysis tell us about what happens in solution? *Molecules, 26*, 6009. https://doi.org/10.3390/molecules26196009

Wu, J., Zang, M., Wang, S., Zhao, B., Bai, J., Xu, C., et al. (2023). Nisin: From a structural and meat preservation perspective. *Food Microbiology, 111*, Article 104207. https://doi.org/10.1016/j.fm.2022.104207

Zehetmeyer, G., Meira, S. M. M., Scheibel, J. M., de Oliveira, R., Bof, V., Brandelli, A., et al. (2016). Influence of melt processing on biodegradable nisin-PBAT films intended for active food packaging applications. *Journal of Applied Polymer Science, 133*, Article 43212. https://doi.org/10.1002/app.43212

Zia, K. M., Barikani, M., Bhatti, I. A., Zuber, M., & Barmar, M. (2009). XRD studies of UV-irradiated chitin based polyurethane elastomers. *Carbohydrate Polymers, 77*, 54–58. https://doi.org/10.1016/j.carbpol.2008.12.002